ISSN 1330-3651 (Print), ISSN 1848-6339 (Online) https://doi.org/10.17559/TV-20221003112627
Original scientific paper

PI/PID Controller Relay Experiment Auto-Tuning with Extended Kalman Filter and Second-Order Generalized Integrator as Parameter Estimators

Danijel PAVKOVIĆ, Dragutin LISJAK, Davor KOLAR*, Mihael CIPEK

Abstract: This paper presents a method for the estimation of key parameters of limit cycle oscillations (amplitude and frequency) during a relay experiment used for automatic tuning of proportional-integral (PI) and proportional-integral-derivative (PID) feedback controllers. The limit cycle parameter estimator is based on the first-order extended Kalman filter (EKF) for resonance frequency estimation, to which a second-order generalized integrator (SOGI) is cascaded for the purpose of limit cycle amplitude estimation. Based on thus-obtained parameters of the limit cycle oscillations, the ultimate gain and the ultimate period of the limit cycle oscillations are estimated. These are subsequently used for the tuning of PI and PID controller according to Takahashi modifications of Ziegler-Nichols tuning rules. The proposed PI and PID controller auto-tuning method is verified by means of simulations and experimentally on the heat and air-flow experimental setup for the case of air temperature feedback control. The results have shown that the proposed auto-tuning system based on relay control experiment for the heat and air-flow process PI/PID temperature control can capture the ultimate gain and period parameters fairly quickly in simulations and in experiments. Subsequent controller tuning according to Takahashi modifications of Ziegler-Nichols rules using thus-obtained ultimate point parameters can provide favourable closed-loop load disturbance rejection, particularly in the case of PID controller.

Keywords: auto-tuning; experimental verification; extended Kalman filter; PI and PID controllers; relay experiment; second-order generalized integrator; Takahashi tuning rules

1 INTRODUCTION (Introductory remarks)

Control objects such as those associated with heat and fluid flow are typically characterized by lag (aperiodic) dynamics and pure delay (dead-time), for which a first-order proportional model with dead-time (FOPDT) process model is frequently used in control system design [1, 2], wherein proportional-integral (PI) and proportional-integral-derivative (PID) controllers are frequently used for that purpose [3-5]. For these types of processes, the Ziegler-Nichols tuning rules for PID controllers are still used in practical applications due to their simplicity [5, 6]. Since the application of Ziegler-Nichols tuning rules typically entails experimental identification of key characteristics of the controlled plant, this controller tuning process is usually automated (automatic tuning or auto-tuning approach), with two characteristic identification experiments typically considered in practical applications:

1. *Process step response-based identification* of a FOPDT model combined with an appropriate tuning approach [7, 8], or a more comprehensive higher-order model [9, 10] which is able to capture the process model transient behaviour more accurately. The latter approach may allow for straightforward tuning of closed-loop damping by using PID controller design based on magnitude optimum [11] or damping optimum [10], even when using more advanced PID-type controller structures [12].
2. *Relay controller-based experiment* to find the process ultimate point, characterized by relay controller equivalent gain (ultimate gain) for which the closed-loop system establishes limit cycle oscillations with steady magnitude and frequency (so-called ultimate frequency) [13, 14], which is typically followed by the use of empirical rules for PID-type controller design [15].

In terms of implementation complexity, the former (step response-based) methods typically require additional signal processing, and may also require high-magnitude experiments, which may need to be repeated to average out the effects of external disturbances [9]. This also indicates that process state (output) needs to be monitored in order to avoid exceeding safe operating limits [15]. On the other hand, the relay control experiment inherently maintains the process operating point in the vicinity of the pre-defined target value [16]. Auto-tuning approaches combining both the time-domain and frequency-domain modelling and identification, try to take advantage of both aforementioned approaches for control system design, wherein a combination of relay experiment and step response identification can be used for control system design [17]. Obviously, auto-tuning PID control is still a propulsive research and development field [6], with a wide range of PID controller auto-tuning solutions having been fielded [18].

Research in relay experiment-based auto-tuning typically focuses on several practical aspects of PID-type controller design. One way to obtain improved closed-loop performance compared to traditional Ziegler-Nichols tuning rules is by controller re-design in order to satisfy the predefined requirements on the closed-loop phase margin. In that sense, reference [19] proposes an improved version of phase margin tuning approach using relay experiment for closed-loop process model identification. A two-relay experiment has been used in [20] to obtain a straight-line approximation the process frequency characteristic in the vicinity of the cross-over frequency thus improving the accuracy of phase margin-based PID controller tuning. A refinement of phase margin-based tuning, proposed in [21], relies on iterative PID controller retuning based on variation of the additional time delay (dead-time) parameter. An alternative approach to identification of characteristic points on the process model frequency characteristic (Nyquist or Bode plots) in the vicinity of the cross-over frequency is by using time-delay filtering of process input and output in real-time during a modified relay experiment [22, 23], or process input and output integration [24]. Some other refinements of the relay-feedback auto-tuning experiment may include: (i) identification of parameters of the second-order

proportional model with dead time (SOPDT) [25], (ii) using an asymmetric relay function in order to estimate in real time the process model gain and normalized dead-time [26], and (iii) using evolutionary algorithms [27, 28] or particle swarm optimization type search [29] to find the optimal PID controller parameters based on suitable cost function. Unfortunately, most of these auto-tuning algorithms require considerable amount of time and computing power to obtain the final result, which may not be suitable for practical applications.

Having this in mind, this paper presents an auto-tuning algorithm for PID-type controller that implements straightforward and low computational load techniques for the estimation of the basic set of parameters for PID controller design. A combined approach to the estimation of limit-cycle resonance frequency and amplitude is proposed, which uses an extended Kalman filter (EKF) [30, 31] as the estimator of free oscillator model resonance frequency, cascaded to a second-order generalized integrator (SOGI) filter [32] used as the estimator of the limit-cycle oscillations amplitude, with both estimators having a relatively low complexity and computational load. Based on the estimated limit-cycle oscillation parameters, Takahashi modifications of Ziegler-Nichols rules [33] are used for subsequent tuning of discrete-time PI and PID controllers. To illustrate the effectiveness of the proposed auto-tuning procedure, it has been verified both by means of computer simulations and experimentally on the temperature and air-flow control test bench for the case of temperature control.

The paper is organized as follows. Section 2 presents the nonlinear dynamic model of the controlled plant (process) in the form of heat and air-flow test bench, which is used for simulation analysis. Section 3 outlines the temperature control system design based on discrete-time (digital) PI and PID feedback controllers and the relay experiment-based auto-tuning procedure suitable for implementation of Takahashi-modified Ziegler-Nichols tuning rules, along with the limit-cycle parameter estimator using EKF and SOGI for combined estimation of oscillations frequency and amplitude. Simulation and experimental verification of the proposed auto-tuning algorithm is presented in Section 4, while concluding remarks and possibilities for future research are given in Section 5.

2 DESCRIPTION OF THE CONTROLLED PLANT

This section outlines the heat and air-flow test bench as the controlled plant (process) in this study and presents the second-order nonlinear process model used in subsequent simulation analysis.

2.1 Heat and Air-Flow Test Bench

Fig. 1 shows the experimental setup of the computer-controlled heater-blower developed in [34], wherein the control is facilitated through a Pentium-based computer equipped with appropriate acquisition and control card [35]. The setup comprises a speed-controlled low-power brushless DC motor with its dedicated power amplifier which drives the ventilation tube air intake fan. The air is then heated by an electric heater, whose power output is controlled by means of a single-phase thyristor power converter. The output air flow (air speed) and air temperature are measured by means of a rotating vane-type flow sensor and a thermocouple, respectively. Output signals from sensors are conditioned by means of appropriate signal amplifiers, which are equipped with analog low-pass filters in order to suppress the process noise/electromagnetic interference (e.g. due to 220 V/50 Hz AC power supply and related thyristor switching action), thus also serving as anti-aliasing filters for sampled process signals.

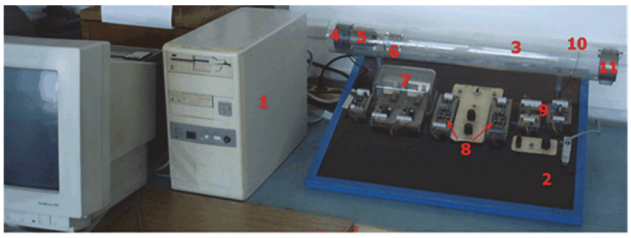

Legend: 1 – Pentium-based PC equipped with acquisition/control card, 2 – setup stand, 3 – blower tube, 4 – speed-controlled fan, 5 – main heater, 6 – auxiliary heater, 7 – power amplifiers, 8 - standalone analog temperature/flow controllers, 9 – sensor amplifiers w/ filters, 10 – thermocouple temperature sensor, 11 – rotating vane-type flow sensor

Figure 1 Heat and air-flow experimental setup

2.1 Process Model

Block diagram representation of the nonlinear dynamic model of the controlled plant (process model is shown in Fig. 2a). The process model comprises a nonlinear static characteristic (Fig. 2b) of the thyristor-based heater power control system which delivers its heat flux to the air-flow being driven through the tube by the speed-controlled fan (Fig. 1).

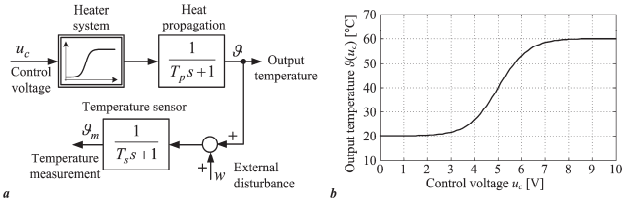

Figure 2 Block diagram representation of controlled plant (a), and temperature vs. control voltage static characteristic (b)

The linear part of the system, i.e. the heat transfer dynamics model and temperature sensor dynamics, are both described by first-order lag terms, whose parameters have been obtained in [34] by means of experimental identification for the case of constant air-flow and ambient air temperature of 20 °C. The parameters of the linear part of the process model that are used in subsequent simulation analysis are as follows: T_p = 16.3 s, and T_s = 18.7 s. The external disturbance within the process model in Fig. 2 represents the action of the auxiliary heater at the experimental setup (see item 6 in Fig. 1), which can be manually turned on/off, thus acting as a disturbance source to the main thyristor-controlled heater system.

3 CONTROL SYSTEM DESIGN

This section presents the discrete-time PID and PI feedback controllers for temperature control and outlines the relay auto-tuning experiment which is the basis for PI/PID controller tuning according to Takahashi-modified Ziegler-Nichols tuning rules. The limit cycle oscillations

parameter estimator, comprising an extended Kalman filter (EKF) as resonance frequency estimator and second-order generalized integrator (SOGI) as estimator of limit-cycle oscillations amplitude, are also presented.

3.1 Discrete-Time PI and PID Controllers

In this work modified PI and PID feedback controller structures are used [33] that are shown in Fig. 3 (i.e. the so-called I + P and I + PD controller). In contrast to the traditional PI and PID controllers, whose proportional (P), integral (I), and derivative (D) actions are all placed into the path of the control error e, in the case of modified controllers, the proportional and derivative actions are conveniently re-arranged to act upon the feedback variable ϑ_m only (Fig. 3).

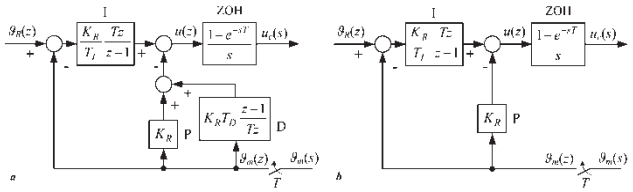

Figure 3 Block diagram of discrete-time PID controller (a) and PI controller (b) with zero-order-hold element (D/A converter) at controller output

In this way, modified controller structures do not introduce additional controller zeros into the closed-loop transfer function, thus avoiding potentially excessive control efforts related to sudden changes of the target value ϑ_R changes or the amplification of noise in the reference value (which would be especially problematic in the case of derivative action of the conventional PID controller). However, should the traditional PID controller structure be preferred, a low-pass filter (prefilter) should be added into the path of the temperature reference (target value) ϑ_R in order to avoid aforementioned excessive control actions. Note also that in order to avoid possible occurrence of large step response overshoots for large reference changes (the so-called integrator windup problem), the controller integral term should be limited when controller output saturation is performed, e.g., by using the so-called reset-integrator method [36].

3.2 Outline of the Relay Auto-Tuning Experiment

The controller auto-tuning corresponds to the case when the controller parameters are calculated by an appropriate tuning algorithm at the demand from the operator, i.e. periodic/sporadic tuning is performed based on the operator's discretion. Typically, the operator monitors the behaviour (performance) of the control system and gives the auto-tuning command when the control system performance worsens, e.g., when the control system response becomes too slow or too oscillatory, which is typically caused by the variations of process parameters [15].

In the closed-loop relay experiment [16], the closed-loop system with constant reference (targe) value ϑ_R is forced to enter the limit-cycle oscillations under a relay-type controller (Fig. 4a) characterized by the peak-to-peak magnitude of relay output change $2U_{\max}$ (Fig. 4b) with respect to the change of sign of the control error signal e. As a result, the controlled plant and controller output are ideally characterized by limit-cycle oscillations with fixed-valued peak-to-peak magnitude $2A$ of the process output (feedback) variable ϑ_m (and control error e), while the bi-level control action the relay controller produces square wave pulsations of the control variable u_c (Fig. 4c) These limit-cycle oscillations of both the process output ϑ_m and controller output u_c are characterized by a fixed frequency Ω (the so-called ultimate frequency), from which the so-called ultimate period T_u is calculated as follows (Fig. 4c):

$$T_u = 2\pi / \Omega \tag{1}$$

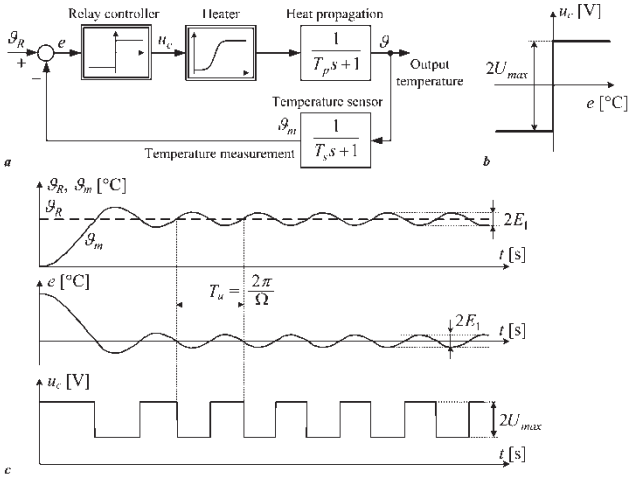

Figure 4 Block diagram of relay feedback control system (a), relay controller static characteristic (b), and typical control system traces during the relay experiment (c)

The equivalent ultimate gain K_u of the relay term, corresponding to the so-called critical gain of the equivalent proportional controller which facilitates closed-loop system limit-cycle oscillations is determined by the so-called harmonic equilibrium method [37]. It is based on the harmonic series approximation of the dominant closed-loop limit-cycle dynamics, for the case when the nonlinear (relay) term is fed harmonic excitation (control error e):

$$e(t) = E_1 \sin(\Omega t) \tag{2}$$

where E_1 is the amplitude and Ω is the frequency of harmonic limit cycle oscillations in the process output ϑ_m (control error e).

For such an excitation at the relay term input, its discontinuous output u_c may be approximated by the following harmonic (Fourier) series:

$$u_c(t) = U_0 + \sum_{n=1}^{\infty} \left[A_n \cos(n\Omega t) + B_n \sin(n\Omega t) \right] \tag{3}$$

where U_0 is the DC component (DC offset) and A_n and B_n are coefficients of the harmonic series (Fourier) expansion, n is the number of the higher-order harmonic component with respect to the principal component at the frequency Ω ($n = 1$).

Due to process dynamics having a low-pass filtering characteristic, the higher-order harmonic components

($n \geq 1$) are effectively suppressed (attenuated), and only the principal component and DC offset are present [15]:

$$u_c(t) = U_0 + A_1 \cos(\Omega t) + B_1 \sin(\Omega t) = \\ = U_0 + U_{\max} \sin(\Omega t + \phi_1) \tag{4}$$

For the simple relay term in Fig. 2b, the ratio between the process output oscillations magnitude and the magnitude of controller output oscillations (representing the ultimate gain value K_u) is obtained as follows [15]:

$$K_u = \frac{4U_{\max}}{E_1 \pi} \tag{4}$$

3.3 Takahashi Tuning Rules and Sampling Time Choice

Takahashi tuning rules represent a modification of the well-known Ziegler-Nichols tuning rules for the case of discrete-time (digital) PID-type controller, wherein the controller sampling time T is also accounted for during the controller design [33]. Thus-modified Ziegler-Nichols expressions for the PI and PID controller and the case of limit-cycle experiment being used to identify the key parameters of the process model are listed in Tab. 1.

The sampling time is chosen based on the a-priori known frequency characteristic of the temperature sensor (Fig. 2a), whose low-pass filtering characteristic also provides anti-aliasing filtering of the measurement signal. Based on this approach, the sampling time is chosen with respect to the sensor bandwidth $\Omega_s = 1/T_s$ of the measurement filter (sensor) as follows:

$$T << T_s \tag{6}$$

which should also comply with the following requirement on the sampling time related to the ultimate period T_u [33]:

$$T \leq 2T_u \tag{7}$$

Table 1 Tuning rules for PI and PID controller parameters based on Takahashi modification of Ziegler-Nichols tuning rules and limit-cycle auto-tuning experiment [33]

Controller	Proportional gain K_R	Integral time constant T_I	Derivative time constant T_D
PI	$K_R = \frac{9}{20} K_u \left(1 - \frac{3}{5}\frac{T}{T_u}\right)$	$T_I = \frac{5}{6} T_u \left(1 - \frac{3}{5}\frac{T}{T_u}\right)$	-
PID	$K_R = \frac{3}{5} K_u \left(1 - \frac{T}{T_u}\right)$	$T_I = \frac{T_u}{2}\left(1 - \frac{T}{T_u}\right)$	$T_D = \frac{T_u}{8}\left(1 - \frac{T}{T_u}\right)^{-1}$

3.4 Estimator of Limit Cycle Oscillations Frequency and Amplitude

For the purpose of on-line estimation, the limit-cycle oscillations are modeled by a simplified model of free oscillator:

$$\frac{d^2 e}{dt^2} + \Omega^2 e = 0 \tag{8}$$

where e represents the control error under relay controller (Fig. 4), and Ω is the oscillator natural frequency to be estimated. Since actual limit-cycle oscillations of the control error may also comprise a small DC bias [16], the control error is passed through a high-pass filter with low cutoff frequency Ω_{bw}, chosen such so as to suppress the DC component while having a large bandwidth (see Fig. 5a).

The discrete-time (digital) implementation of the free oscillator model in equation (8) rewritten in terms of high-pass filtered control error e_F reads as follows:

$$e_F(k) = h(k) = 2e_F(k-1)\cos(\Omega T) - e_F(k-2) \tag{9}$$

where $h(k)$ is the nonlinear function comprising past states of the measurement signal e_F and the natural frequency Ω of the free oscillator, T is the discrete-time error signal sampling time and k is the sampling step.

The above dynamic model is implemented within an extended Kalman filter (EKF) which serves as a recursive algorithm of parameter estimation optimal in the least-squares sense [30, 31]. The recursive equations for the first-order EKF estimator read as follows:

$$P(k) = \left[1 - K(k-1)H(k-1)\right]P(k-1) + Q(k-1) \tag{10}$$

$$H(k) = \frac{\partial h\left[\hat{\Omega}(k-1), e_F(k-1), e_F(k-2)\right]}{\partial \hat{\Omega}(k-1)} = \\ = -2Te_F(k-1)\sin[\hat{\Omega}(k-1)T] \tag{11}$$

$$K(k) = P(k)H(k) / P(k)H^2(k) + R(k) \tag{12}$$

$$\varepsilon(k) = e_F(k) - h\left(\hat{\Omega}(k-1), e_F(k-1), e_F(k-2)\right) = \\ = e_F(k) - 2e_F(k-1)\cos(\hat{\Omega}(k-1)T) + e_F(k-2) \tag{13}$$

$$\hat{\Omega}(k) = \hat{\Omega}(k-1) + K(k)\varepsilon(k) \tag{14}$$

where Q is the desired variance of perturbations in the estimated parameter Ω, R is the noise variance in the measurement signal (control error), P is the Kalman filter error variance, K is the estimator update gain, H is the gain of the output equation $h(k)$ linearized in the vicinity of the estimated frequency of limit cycle oscillations $\hat{\Omega}$.

In order to simplify the parameter estimator design, the measurement noise variance R can be set to unit value (R = 1), and the EKF-based tuning is performed by varying the desired variance Q of the estimated frequency parameter Ω perturbations [38].

Fig. 5a shows the overall block diagram representation of the above scalar (first-order) EKF estimator of the limit cycle resonance frequency Ω, whereas Fig. 5b shows the principal representation of the limit cycle amplitude

estimator. In the latter case the high-pass filtered error signal e_F is forwarded to so-called second-order generalized estimator (SOGI) [32], which is capable of reconstructing both the direct (in-phase) error component e_d and its orthogonal counterpart e_q (delayed in phase by $\pi/2$) in the vicinity of its band-pass frequency $\hat{\Omega}$ (provided by the EKF estimator). Using the aforementioned direct and quadrature signals, the estimated amplitude $\hat{E}_1$ of the error signal can be obtained as follows:

$$\hat{E}_1 = \sqrt{e_d^2 + e_q^2} \tag{15}$$

which is valid for e_d and e_q being orthogonal harmonic signals with the same amplitude.

Fig. 6a shows the realization of the adaptive discrete-time SOGI estimator, with the central frequency updated by means of the previously described EKF estimator. Its linear time-invariant (LTI) form is shown in Fig. 6b, which can be used to derive the following SOGI band-pass filter transfer function model [39]:

$$G_{BP}(s) = \frac{e_d(s)}{e_F(s)} = \frac{K_I \hat{\Omega} s}{s^2 + K_I \hat{\Omega} s + \hat{\Omega}^2} = \\ = \frac{2\zeta \hat{\Omega} s}{s^2 + 2\zeta \hat{\Omega} s + \hat{\Omega}^2} \tag{16}$$

where K_I is the SOGI filter feedback gain parameter and ζ is the filter damping ratio which is typically set to $\zeta > 0.5$, thus guaranteeing a well-damped band-pass filter transient response. Since the SOGI band-pass filter is adapted with respect to the estimated resonance frequency Ω, its gain is unit valued at that particular frequency, thus resulting in accurate estimation of limit-cycle oscillations amplitude and good selectivity of the principal component of limit cycle oscillations.

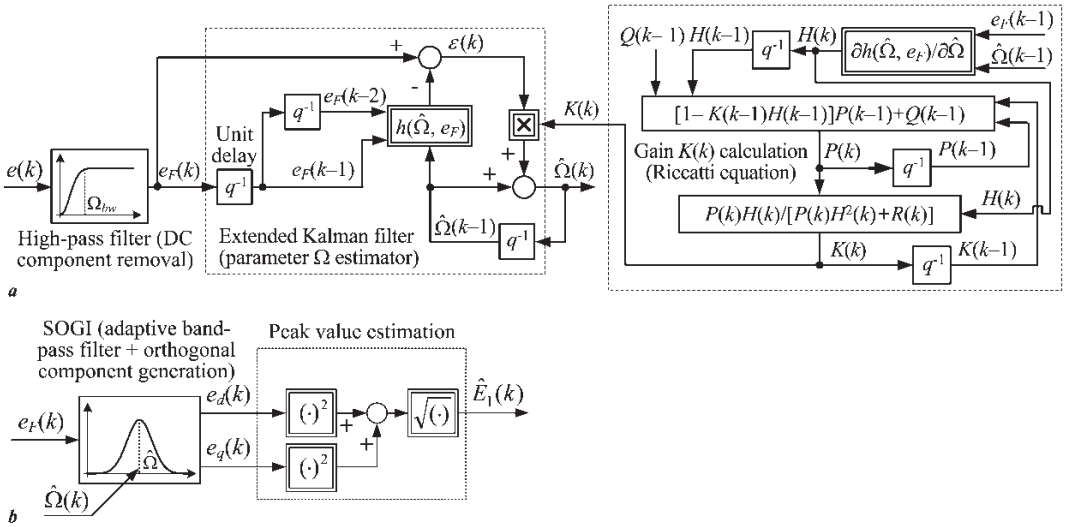

Figure 5 Block diagram representation of EKF-based limit-cycle oscillation frequency estimator (a), and principle of SOGI-based limit cycle amplitude estimator (b)

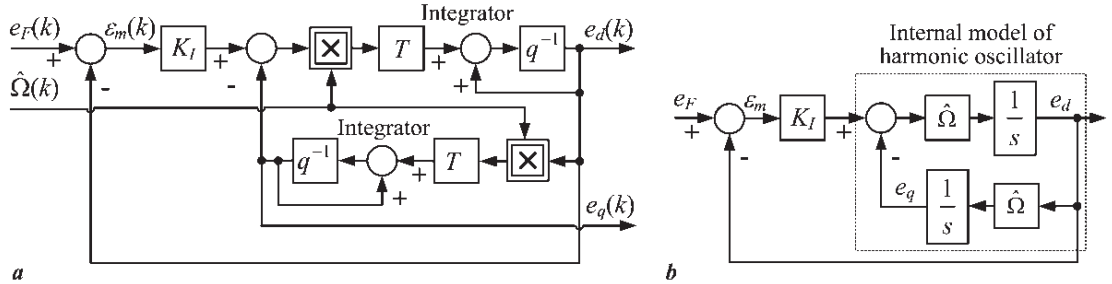

Figure 6 Adaptive discrete-time SOGI estimator of direct and quadrature control error signal components (a) and its linear time-invariant counterpart (b)

4 PI/PID CONTROLLER SIMULATION AND EXPERIMENTAL VERIFICATION

The effectiveness of the proposed PI/PID controller auto-tuning is validated first by means of simulations, followed by experimental verification on the dedicated heat and air-flow experimental setup.

4.1 Comparative Simulation Results

The simulation verification of the proposed auto-tuning control system for the PI and PID controller has been carried out using the dynamic model of the controlled plant (process) described in Section 2. The limit-cycle oscillations parameter estimator (EKF plus SOGI algorithm) has been tuned with the following values of tuning parameters: $R = 1$, $Q = 1$, $K_I = 2$ ($\zeta = 1$), with the sampling time T for the auto-tuning algorithm and PI/PID controllers being $T = 1$ s. The simulation scenario begins with the auto-tuning algorithm being executed in the first stage (t = 0-200 s) wherein the relay controller temperature reference ϑ_R is set to 40 °C. After the auto-tuner has identified the parameters of the limit-cycle oscillations (indicated by settling of their values), the auto-tuned PI or

PID controller is turned on, thus testing the effectiveness of closed-loop control. In order to test the disturbance suppression ability of the feedback loop, the external disturbance w = 3 °C is turned on at t = 350 s. Figs. 7 and 8 show the results of the PI and PID controller auto-tuning test, respectively.

During the first stage of the auto-tuner test (t = 0-200 s), relay controller feedback is established and the output variable (air temperature measurement ϑ_m) is quickly brought in the vicinity of the target value ϑ_R and limit-cycle oscillations are successfully established after a short (40 seconds long) transient. During this initial response transient, the parameter estimator has been disabled to avoid unnecessary and excessive perturbations in the estimated limit-cycle oscillation parameters, which might otherwise occur due to abrupt and large magnitude variations of the process output. The traces of estimated limit-cycle oscillations parameters, shown in Figs. 7b and 8b) are characterized by rather fast responses, with steady-state parameter values being reached within approximately 90 s, and their steady-state responses being characterized by negligible perturbations, which points out to favorable parameter estimator tuning. The closed-loop responses of feedback control systems with PI and PID controller are shown in Figs. 7a and 8a, respectively. The PID controller-based closed-loop responses (Fig. 7a) are characterized by more favorable closed-loop damping and response settling time when compared to the case when PI feedback controller is used (Fig. 8a), both after the auto-tuning test and for the case when stepwise external disturbance w = 3 °C is applied. This can be attributed to: (i) stabilizing action of the derivative term of the PID controller, thus having an additional degree of freedom in closed-loop dynamics tuning when compared to the PI feedback controller, and (ii) inherent characteristic of the Ziegler-Nichols tuning rules which typically allow for weaker closed-loop damping in order to achieve faster disturbance response and, consequently, improved disturbance suppression ability [33].

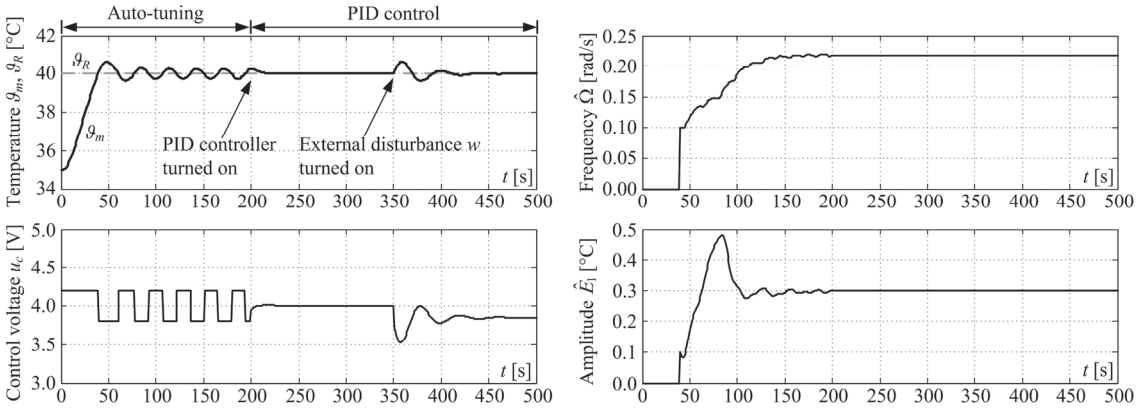

Figure 7 Simulation results of auto-tuning relay experiment followed by temperature PID feedback control (a) and results of limit-cycle oscillations frequency and amplitude estimation (b)

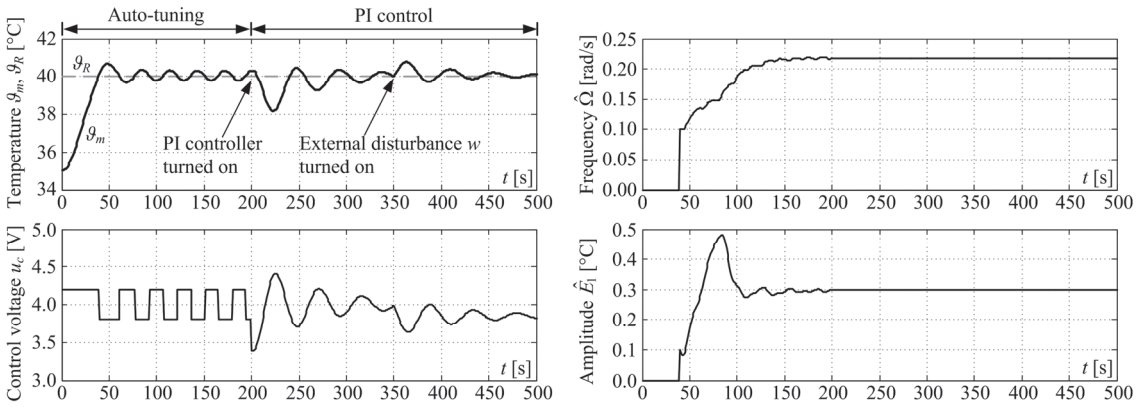

Figure 8 Simulation results of auto-tuning relay experiment followed by temperature PI feedback control (a) and results of limit-cycle oscillations frequency and amplitude estimation (b)

4.2 Comparative Experimental Results

Figs. 9 and 10 show the comparative experimental responses of the auto-tuning PI and PID controller for the case of temperature reference set to ϑ_R = 40 °C, where the experimental test scenario closely matches the simulation verification scenario of the auto-tuning PI/PID controller in Figs. 7 and 8. The experimental results in Figs. 9 and 10 confirm that the proposed damping optimum-based PI/PID controller auto-tuning method results in a consistent estimation of limit-cycle oscillations parameters during the auto-tuning test (Figs. 9b and 10b), and relatively well-damped response of the closed-loop system in the case of PID controller (Fig. 10a), whereas the damping of the feedback control system comprising the PI controller is characterized by less favorable damping due to the previously mentioned absence of the derivative term stabilizing action. It should be noted that the resonance frequency and amplitude of limit cycle oscillations differ somewhat from the simulation, which is due to: (i) setting

of the air-flow propeller reference speed being manually adjusted to achieve steady air flow, and (ii) higher magnitude of the control voltage stepwise change within the relay term (U_{max} = 1 V), which was chosen as a compromise between the sensitivity to temperature measurement noise and achieving ample magnitude of temperature measurement variations during the relay control auto-tuning test.

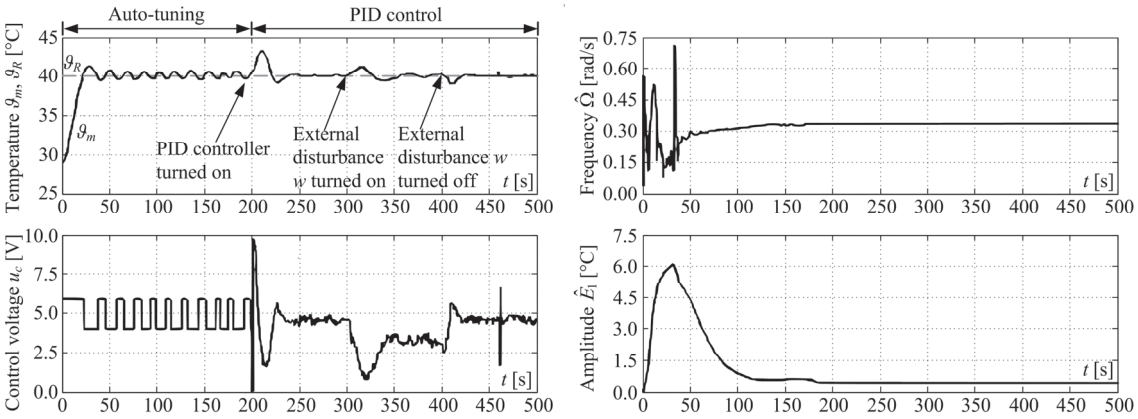

Figure 9 Experimental results of auto-tuning relay experiment followed by temperature PID feedback control (a) and results of limit-cycle oscillations frequency and amplitude estimation (b)

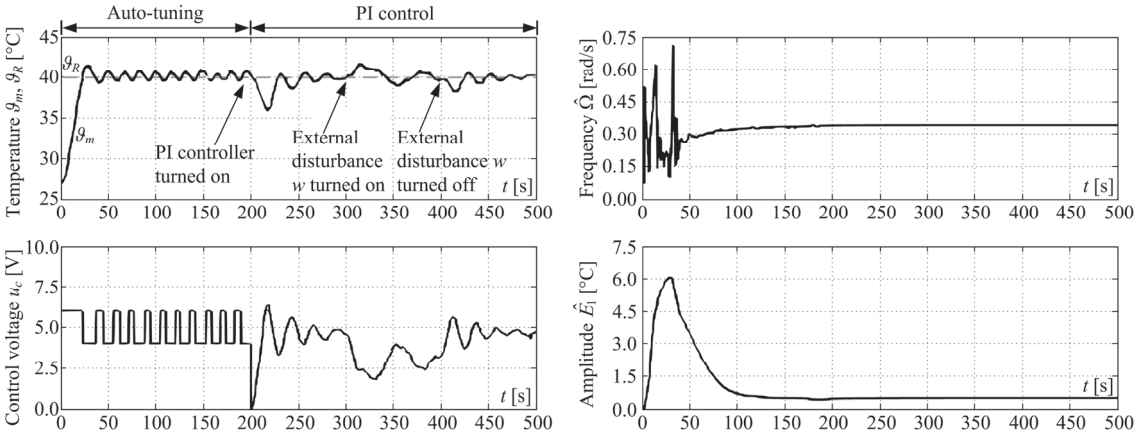

Figure 10 Experimental results of auto-tuning relay experiment followed by temperature PI feedback control (a) and results of limit-cycle oscillations frequency and amplitude estimation (b)

5 CONCLUSION

The paper has presented a novel estimator of limit-cycle oscillations amplitude and frequency during a relay experiment, which has been used for automatic tuning of PI and PID feedback controllers. The proposed limit cycle parameter estimator has included the EKF-based limit-cycle resonance frequency estimator and the associated second-order generalized integrator (SOGI) for the estimation of limit-cycle oscillations amplitude, with both estimators having a relatively low complexity and computational load. Thus obtained limit-cycle parameters have been used to determine the parameters of the closed-loop ultimate point, i.e. the ultimate gain of the relay controller and the ultimate period of limit-cycle oscillations, which have been subsequently used for the tuning of PI and PID controllers according to Takahashi modifications of Ziegler-Nichols tuning rules. The proposed PI and PID controller auto-tuning method has been verified by means of simulations and experimentally for the case of air temperature feedback control on the heat and air-flow experimental setup.

The simulation and experimental results have shown that the estimator of limit-cycle oscillations parameters is characterized by rather fast response, with steady-state parameter values having been reached within approximately 90 s, in both simulations and experiments. The steady-state values of estimated natural frequency and amplitude parameters in both simulations and experiments are characterized by negligible perturbations, which points out to favorable suppression of high-frequency "noise" within the EKF and SOGI-based estimator. This is especially important in the case of experimental tests, characterized by larger magnitudes of relay control action during the ultimate point parameter estimation phase.

The closed-loop responses of PI and PID feedback controller-based systems tuned according to Takahashi rules following the relay feedback auto-tuning experiment have indicated that experimental tests auto-tuned PI and PID feedback controller generally comply rather well with simulation results. In particular, the PID controller-based closed-loop system has been characterized by substantially improved closed-loop damping and response settling time compared to the case when the PI feedback controller has been used. For the particular heat and air-flow process and stepwise temperature disturbance in the process steady-state, typical settling times obtained when PID controller is used are about 50 s, whereas the PI controller-based system is characterized by more oscillatory response with settling times of about 150 s (three times slower settling). The main

advantage of PID controller use is its additional ability to condition the closed-loop system dynamics via its derivative action (which is not present in the PI controller), thus facilitating faster settling and improving the closed-loop stability margin.

The aforementioned is especially important when controller auto-tuning is based on semi-empirical Ziegler-Nichols type rules, because they typically allow for weaker closed-loop damping in order to obtain faster disturbance response. In that sense, the PID controller should be preferred due to the additional stabilizing action of the derivative term that should improve the damping characteristic of the closed-loop system and should result in closed-loop system disturbance rejection performance that is both faster and better damped compared to the case when PI controller is used.

Acknowledgements

It is gratefully acknowledged that this research has been supported by the European Regional Development Fund (ERDF) through the grant KK.01.1.1.07.0031 "Prognostic maintenance of industrial rotary equipment based on machine learning and IoT technology in interaction with information systems".

Nomenclature

Abbreviations:

EKF	Extended Kalman filter
FOPDT	First-order Proportional model with Dead Time
max	Maximum value
PI	Proportional-integral (controller)
PID	Proportional-integral-derivative (controller)
PLC	Programmable logic controller (control unit)
SOGI	Second-order generalized integrator (band-pass filter)
SOPDT	Second-order Proportional model with Dead Time

Variables:

e, e_F	Control error signal and its high-pass filtered value
e_d, e_q	Direct and orthogonal component of high-pass filtered control error value
$\hat{E}_1$	Control error signal principal component amplitude estimated value
$h(k)$	EKF output nonlinear function
$H(k)$, $H(k-1)$	EKF gain parameter of the linearized output equation $h(k)$
$K(k)$, $K(k-1)$	EKF time-varying gain parameter
$P(k)$, $P(k-1)$	EKF time-varying error variance parameter
$R(k)$	EKF measurement noise variance parameter
$Q(k-1)$	EKF state perturbation variance parameter
q^{-1}	Discrete-time operator of unit time delay (one step delay)
s	Laplace variable
ε	EKF estimator tracking error
ε_m	SOGI estimator tracking error
$\hat{\Omega}$	Estimated frequency of limit-cycle oscillations

Parameters:

A_1, B_1	Coefficients of principal component approximation of relay controller output
A_n, B_n	Coefficients of harmonic (Fourier) series approximation of relay controller output
U_0, $U_{\max}$	DC offset (bias) and amplitude of the principal component of the relay controller output
K_I	SOGI estimator gain parameter
K_R, T_I, T_D	Proportional gain, integral time constant and derivative time constant
K_u, T_u	Ultimate gain (of the relay term) and ultimate period of limit-cycle oscillations
T	Sampling time
φ_1,φ_n	Principal component phase shift and n-th harmonic component phase shift
Ω	Limit-cycle resonance frequency
ζ	Damping ratio

Symbols:

$\wedge$	Estimated value

6 REFERENCES

[1] Bonivento, C., Castaldi, P., & Mirotta, D. (2001). Predictive Control vs. PID Control of an Industrial Heat Exchanger. *Proceedings of 9th Mediterranean Conference on Control and Automation*, 6.

[2] Al-Dawery, S. K., Alrahawi, A. M., & Al-Zobai, K. M. (2012). Dynamic Modeling and Control of Plate Heat Exchanger, *International Journal of Heat and Mass Transfer*, *55*(23-24), 6873-5880. https://doi.org/10.1016/j.ijheatmasstransfer.2012.06.094

[3] Åström, K. J. & Hägglund, T. (2001). The Future of PID Control. *Control Engineering Practice*, *9*(11), 1163-1175. https://doi.org/10.1016/S0967-0661(01)00062-4

[4] Panda, R. C., Yu, C.-C., & Huang, H.-P. (2004).PID Tuning Rules for SOPDT systems: Review and Some New Results. *ISA Transactions*, *43*(2), 283-295. https://doi.org/10.1016/S0019-0578(07)60037-8

[5] Åström, K. J. & Hägglund, T. (2004). Revisiting the Ziegler-Nichols Step Response Method for PID Control. *Journal of Process Control*, *14*(6), 635-650. https://doi.org/10.1016/j.jprocont.2004.01.002

[6] Leva, A., Negro, S., & Papadopoulos, A.V. (2010). PI/PID Autotuning with Contextual Model Parametrisation. *Journal of Process Control*, *20*(4), 452-463. https://doi.org/10.1016/j.jprocont.2010.01.005

[7] Villanova, R. (2008). IMC based Robust PID design: Tuning Guidelines and Automatic Tuning. *Journal of Process Control*, *18*(1), 61-70. https://doi.org/10.1016/j.jprocont.2007.05.004

[8] Leva, A. (2007). Comparative Study of Model-based PI(D) Autotuning Methods. *Proceedings of the 2007 American Control Conference*, 5796-5801. https://doi.org/10.1109/ACC.2007.4282602

[9] Vrančić, D., Peng, Y., & Strmčnik, S. (1999). A New PID Controller Tuning Method Based on Multiple Integrations, *Control Engineering Practice*, *7*(5), 623-633. https://doi.org/10.1016/S0967-0661(98)00198-1

[10] Pavković, D., Polak S., & Zorc, D. (2014).PID Controller Auto-Tuning Based on Process Step Response and Damping Optimum Criterion. *ISA Transactions*, *53*(1), 85-96. https://doi.org/10.1016/j.isatra.2013.08.011

[11] Vrančić, D., Strmčnik, S., & Juričić, Đ. (2001). A Magnitude Optimum Multiple Integration Tuning Method for Filtered PID Controller. *Automatica*, *37*(9), 1473-1479. https://doi.org/10.1016/S0005-1098(01)00088-7

[12] Vrančić, D. & Huba, M. (2021). High-Order Filtered PID Controller Tuning Based on Magnitude Optimum. *Mathematics*, *9*, 1340, 24. https://doi.org/10.3390/math9121340

[13] Hang, C. C., Åström, K. J., & Wang, Q. G. (2002). Relay Feedback Auto-tuning of Process Controllers - A Tutorial Review. *Journal of Process Control*, *12*(1), 143-162.

https://doi.org/10.1016/S0959-1524(01)00025-7
[14] Åström, K. J. & Hägglund, T. (1995). *PID Controllers: Theory, Design and Tuning*. Research Triangle Park, Durham, NC, USA, Instrument Society of America.
[15] Hagglund, T. & Åström, K. J. (2000). *Automatic Tuning of PID controllers: The Control Handbook*. Boca Raton, FL, USA: CRC Press.
[16] Yu, C. C. *Autotuning of PID controllers - A Relay Feedback Approach*. London, UK, Springer-Verlag.
[17] Bi, Q., Cai, W.-B., Wang, Q.-G., Hang, C.-C., Lee, E.-L., Sun, Y., Liu, K.-D., Zhang, Y., & Zou, B. (2000). Advanced Controller Auto-tuning and its Application in HVAC Systems. *Control Engineering Practice*, *8*(6), 633-644. https://doi.org/10.1016/S0967-0661(99)00198-7
[18] Li, Y., Ang, K.-H., & Chong, G. (2006). Patents, Software and Hardware for PID Control. *IEEE Control Systems Magazine*, *26*(1), 42-54. https://doi.org/10.1109/MCS.2006.1580153
[19] Zeng, D., Zheng, Y., Luo, W., Hu, Y., Cui, Q., Li, Q., & Peng, P. (2019). Research on Improved Auto-Tuning of a PID Controller Based on Phase Angle Margin. *Energies*, *12*, 1704, 16. https://doi.org/10.3390/en12091704
[20] Romero, J. A., Sanchis, R. & Balaguer, P. (2011). PI and PID auto-tuning procedure based on simplified single parameter optimization. *Journal of Process Control*, *21*, 840-851. https://doi.org/10.1016/j.jprocont.2011.04.003
[21] Ho, W. K., Hong, Y., Hansson, A., Hjalmarsson, H., & Deng, J. W. (2003). Relay auto-tuning of PID controllers using iterative feedback tuning. *Automatica*, *39*(1), 149-157. https://doi.org/10.1016/S0005-1098(02)00201-7
[22] Hofreiter, M. (2018). Alternative Identification Method using Biased Relay Feedback. *Proceedings of the 16th IFAC Symposium on Information Control Problems in Manufacturing*, 6. https://doi.org/10.1016/j.ifacol.2018.08.491
[23] Hofreiter, M. (2017). Biased-Relay Feedback Identification for Time Delay Systems, *Proceedings of the 20th IFAC World Congress*, 15185-15190. https://doi.org/10.1016/j.ifacol.2017.08.1740
[24] Jeng, J.-C., Lee, M.-W., & Huang, H.-P. (2005). Identification of Block-Oriented Nonlinear Processes Using Designed Relay Feedback Tests. *Industrial & Engineering Chemistry Research*, *44*(7), 2145-2155. https://doi.org/10.1021/ie049484o
[25] Huang, H.-P., Jeng, J.-C., & Luo, K.-Y. (2005). Auto-tune system using single-run relay feedback test and model-based controller design. *Journal of Process Control*, *15*, 713-727. https://doi.org/10.1016/j.jprocont.2004.11.004
[26] Berner, J., Åström, K. J., & Hägglund, T. (2014). Towards a New Generation of Relay Autotuners. *Proceedings of the 19th IFAC World Congress*, 11288-11293. https://doi.org/10.3182/20140824-6-ZA-1003.01591
[27] Wang, Y., Xu, D., Yang, H., & Zhu, C. (2021). A Fractional Order Proportional-Integral-Derivative Controller for Series Continuous Stirred Tank Reactor System. *Tehnički vjesnik/Technical Gazette*, *28*(4), 1277-1284. https://doi.org/10.17559/TV-20210318100642
[28] Sivadasan, J. & Willjuice Iruthayarajan, M. (2018). Tuning of Nonlinear PID Controller for TRMS Using Evolutionary Computation Methods. *Tehnički vjesnik/Technical Gazette*, *25*(Supplement 1), 94-98. https://doi.org/10.17559/TV-20170612090511
[29] Kong, F., Li, J., & Yang. D. (2021). Optimal Control Strategy of Turbine Governor Parameters Based on Improved Beetle Antennae Search Algorithm. *Tehnički vjesnik/Technical Gazette*, *28*(4), 1082-1090. https://doi.org/10.17559/TV-20201012123041
[30] Grewal, M. S. & Andrews, A. P. (2001). *Kalman filtering - theory and practice*. New York, NY, USA: John Wiley and Sons, Inc.
[31] Banjac, Z. & Kovačević, B. (2022). Robustified Kalman Filtering Using Both Dynamic Stochastic Approximation and M-Robust Performance Index. *Tehnički vjesnik/Technical Gazette*, *29*, (3), 907-914. https://doi.org/10.17559/TV-20200929143934
[32] Xiao, F., Dong, L., Li, L., & Liao, X. (2017). A Frequency-Fixed SOGI-Based PLL for Single-Phase Grid-Connected Converters. *IEEE Transactions on Power Electronics*, *32*(3), 1713-1719. https://doi.org/10.1109/TPEL.2016.2606623
[33] Isermann, R. (1989). *Digital control systems - Volume 1: Fundamentals, Deterministic Control*. Berlin, Germany: Springer-Verlag.
[34] Deur, J., Cvetan, D., & Zorc, D. (1995). Identification and Digital Control of an Air Heater. *40th Anniversary Conference KoREMA*, 427-434.
[35] Advantech Co. (2010). PCL-812PG 30 kS/s, 12-bit, 16-ch ISA Multifunction Card.
[36] Åström, K. J. & Wittenmark, B. (1997). *Computer Controlled Systems - Theory and Design*. Englewood Cliffs, NJ, USA, Prentice Hall.
[37] Slotine J.-J. E. & Li, W. (1991). *Applied Nonlinear Control.* Englewood Cliffs, NJ, USA, Prentice-Hall.
[38] Pavković, D., Deur, J., & Lisac, A. (2011). A Torque Estimator-based Control Strategy for Oil-Well Drill-string Torsional Vibrations Active Damping Including an Auto-tuning Algorithm. *Control Engineering Practice*, *19*(8), 836-850. https://doi.org/10.1016/j.conengprac.2011.04.012
[39] Pavković, D., Kozhushko, Y., Hrgetić, M., Zorc, D., & Cipek, M. (2019). Damping Optimum Design of Single-Phase Inverter Synchronization and Current Control System. *IEEE 39th International Conference on Electronics and Nanotechnology*, 572-577. https://doi.org/10.1109/ELNANO.2019.8783726

Contact information:

Danijel PAVKOVIC, PhD, Associate Professor
University of Zagreb,
Faculty of Mechanical Engineering and Naval Architecture,
Ivana Lučića 5, 10002 Zagreb, Croatia
E-mail: danijel.pavkovic@fsb.hr

Dragutin LISJAK, PhD, Full Professor
University of Zagreb,
Faculty of Mechanical Engineering and Naval Architecture,
Ivana Lučića 5, 10002 Zagreb, Croatia
E-mail: dragutin.lisjak@fsb.hr

Davor KOLAR, PhD
(Corresponding author)
University of Zagreb,
Faculty of Mechanical Engineering and Naval Architecture,
Ivana Lučića 5, 10002 Zagreb, Croatia
E-mail: davor.kolar@fsb.hr

Mihael CIPEK, PhD, Assistant Professor
University of Zagreb,
Faculty of Mechanical Engineering and Naval Architecture,
Ivana Lučića 5, 10002 Zagreb, Croatia
E-mail: mihael.cipek@fsb.hr